

# A MODEL OF SEQUENCE DEPENDENT RNA-POLYMERASE DIFFUSION ALONG DNA.

Maria Barbi\*<sup>†¶</sup>, Christophe Place<sup>#</sup>, Vladislav Popkov<sup>§||</sup>, Mario Salerno<sup>†</sup>

February 25, 2019

<sup>†</sup> Dipartimento di Fisica "E.R. Caianiello" and INFN, Università di Salerno, Baronissi (SA), Italy; <sup>#</sup> Laboratoire de Physique, CNRS-UMR 5672, École Normale Supérieure de Lyon, Lyon, France; <sup>§</sup> Institut für Festkörperforschung, Forschungszentrum Jülich GmbH, Jülich, Germany; <sup>||</sup> Institute for Low Temperature Physics, Kharkov, Ukraine; and <sup>¶</sup> Laboratoire de Physique Theorique des Liquides, Université Paris VI, Paris, France.

## Abstract

We introduce a probabilistic model for the RNA-polymerase sliding motion along DNA during the promoter search. The model accounts for possible effects due to sequence-dependent interactions between the nonspecific DNA and the enzyme. We focus on T7 RNA-polymerase and exploit the available information about its interaction at the promoter site in order to investigate the influence of bacteriophage T7 DNA sequence on the dynamics of the sliding process. Hydrogen bonds in the major groove are used as the main sequence-dependent interaction between the RNA-polymerase and the DNA. The resulting dynamical properties and the possibility of an experimental validation are discussed in details. We show that, while at large times the process reaches a pure diffusive regime, it initially displays a sub-diffusive behavior. The crossover from anomalous to normal diffusion may occur at times large enough to be of biological interest.

## Introduction

The way by which the different proteins can find and recognize their target site along a long DNA chain represents still now a puzzling problem in many cases. These mechanisms can imply jumping or inter-segment transfer and non-specific sliding along the DNA (Travers, 1993; von Hippel and Berg, 1989; Shimamoto, 1999; Stanford *et al.*, 2000). In particular, it has been experimentally shown that sliding along DNA is at least one of the main mechanisms by which RNA-polymerase (RNAP) can find specific DNA sequences: several direct and indirect evidences have been obtained by different kind of experiments (Park *et al.*, 1982a,b; Singer and Wu, 1987; Ricchetti *et al.*, 1988; Kabata *et al.*, 1993; Guthold *et al.*, 1994; Schulz *et al.*, 1998; Guthold *et al.*, 1999; Shimamoto, 1999; Harada *et al.*, 1999). Nevertheless, a precise experimental determination of the statistical law char-

acterizing the diffusive motion of RNAP along DNA during the promoter search, is presently lacking. The knowledge of the statistical properties of the RNAP dynamics is important for giving an insight into the nonspecific interactions that guide the RNA-polymerase along the DNA. This is a field scarcely investigated from an experimental point of view (Shimamoto, 1999) although ongoing single molecule experiments would probably shade some light on this question (Guthold *et al.*, 1999; Shimamoto, 1999; Harada *et al.*, 1999). It is believed that during the sliding motion, the activation barrier for the translocation of the RNAP to contiguous non-specific positions is high enough to randomize the polymerase motion through collisions with the solvent molecules (Shimamoto, 1999), but appropriately small compared to the thermal energy, in order to allow the protein to move (von Hippel and Berg, 1989). This has induced some authors to propose a model where RNAP freely

slides along DNA under the effect of the thermal fluctuations without any sequence dependent interaction, i.e. the DNA is seen as an homogeneous cylinder on which RNAP can diffuse until the promoter site is reached (von Hippel and Berg, 1989; von Hippel *et al.*, 1996). Anyway, since sliding represents the last stage in the promoter search, a recognition mechanism must be involved, i.e. the RNAP must be able to distinguish the promoter region from nonspecific DNA. To this regard, the possibility that sliding could imply sequence dependent RNAP-DNA interactions is rather reasonable. This suggests that DNA base sequence could influence the statistical properties of the diffusive RNAP motion (von Hippel and Berg, 1989) (base sequence induced dynamics along DNA was also considered in Ref.s (Salerno, 1991, 1995)).

The aim of the present paper is to investigate this idea in the context of a simple probabilistic model for the RNA-polymerase sliding along DNA which accounts for the sequence-dependent interactions between the nonspecific DNA and the enzyme. The model is based on the assumption that, in order to test whether some special "signal" associated with the promoter is present, RNAP needs to "read" the underlying sequence while sliding, i.e. a *sequence-dependent interaction* should be at work all during the search. This means that the DNA sequence can influence the dynamics of the polymerase also far from the promoter. In this sense, the stop at the promoter should be the extreme effect of a complex dynamics, i.e. the RNAP should follow a noise-influenced, sequence-dependent motion that includes the possibility of slowing down, pauses and stops. From this point of view the widely accepted assumption of a standard random walk (i.e. with a mean square deviation of the enzyme displacement  $\langle \Delta n^2 \rangle$  linearly dependent on time) of the RNAP along DNA appears to be a practical but incorrect simplification.

As mentioned before, the nature of this "reading" interaction, and therefore its strength and its degree of sequence sensitivity, is unknown: the sequence dependent "signal" could be steric, or mediated by chemical bonds, could depend on the local DNA three-dimensional structure (Travers, 1993) as well as on a specific set of binding sites (Seeman *et al.*, 1976), etc. Thus, for instance, it has been shown that the *E. Coli* RNAP holoenzyme bends DNA in correspondence to the promoter (Schulz *et al.*, 1998), so

that a sensitivity to the local DNA flexibility seems to be involved. In the interaction between the same enzyme and the T7 DNA, nevertheless, direct contacts between the  $\beta$ ,  $\beta'$  and  $\sigma$  sub-units and DNA have been shown, this suggesting their participation in the promoter search (Park *et al.*, 1982a). The recognition is in any case associated with the base-pair sequence, which determines the main structural and chemical characteristics of the corresponding DNA region.

To investigate the possibility of a sequence-dependent diffusive motion of the RNAP along DNA we shall use some crystallographic information about sequence-dependent RNAP-DNA interactions inside the promoter region. Outside the promoter region, in fact, no experimental information exists about this interaction, due to the lower stability of the nonspecific complexes. We shall then extrapolate it by assuming that the enzyme and the DNA try to reproduce the same interaction as in the promoter region. This defines a base sequence energy landscape from which hopping rates of the enzyme on the DNA (viewed as a discrete inhomogeneous lattice) can be deduced. The diffusive motion of the RNAP is then studied by Monte Carlo simulations of the probabilistic process on the landscape energy both in absence and in presence of threshold values which define different rules for the hopping motion. As a result we show that while at large times the process reaches a pure diffusive regime, at the initial stages it displays a sub-diffusive behavior. The crossover from anomalous diffusion to normal diffusion may occur at times large enough to be of biological interest. We will focus on the specific example of the T7 RNA-polymerase sliding on a 3000 bps DNA fragment of the bacteriophage T7.

The paper is organized as follows. In Section 1 we use some known information from crystallography structure of the T7 RNAP-promoter complex to introduce a sequence dependent model for the RNAP-DNA nonspecific interaction. An energy landscape with minima corresponding to the recognition sequence GAGTC inside the promoter is constructed. We then introduce four possible models for the RNAP diffusive motion along DNA by using the sequence induced energy landscape and its modifications, as the inclusion of energy thresholds, which allow to describe different possible reading mechanisms. The rates of translocation to the neighboring

sites are constructed from the energy landscapes ( for the different models) by means of the *Arrhenius law*. In Section 2 we use Monte Carlo simulations to study in detail the different dynamical regimes of our models. Finally, we discuss in Section 3 the limits of our analysis and the possibility to check the results with experiments, so to verify if the inferred mechanism actually corresponds to the real one, and we draw our Conclusions.

## 1 Methods: experimental data and theoretical model

### 1.1 T7 RNAP - DNA interaction and promoter recognition

As mentioned in the Introduction, it is still not well known which kind of sequence-dependent interactions allow the polymerase to test the DNA during the promoter search (Travers, 1993). To our knowledge, there are no experimental investigations about the details of the nonspecific polymerase-DNA complexes. The stability of the RNAP-DNA nonspecific complex is probably mainly due to electrostatic interaction with the backbone phosphate of DNA (von Hippel *et al.*, 1996), i.e. interactions that are not sensible to the specific base-pair composition. On the other hand, the specific *open complex* formed by the RNAP and its target promoter is stable enough to be studied by crystallography. Even if the open complex formation requires a series of conformational rearrangements that may change completely the set of polymerase-DNA interactions, one can suppose that at least some of the interactions observed in the specific complex could be already present during sliding, and might be used in the recognition mechanism. This hypothesis is interesting also if the actual reading mechanism is not exactly the same but of a similar type; the study of the consequent dynamics may help, from a more general point of view, in understanding which kind of sequence-dependent interactions are compatible with the experimental data.

Cheetham, Jeruzalemi and Steitz (Cheetham *et al.*, 1999) give a detailed analysis of the polymerase-promoter open complex for the case of bacteriophage T7, to which we will refer in the following. From the crystallographic analysis, it

emerges that the T7 RNAP interacts with the promoter in three regions <sup>1</sup>. The first interaction is with the AT-rich region between positions -17 to -13 relative to the starting site of transcription. The N-terminal domain of the polymerase enters here in the minor groove of DNA, and the helix appears to be distorted to form a shallower minor groove, so that the recognition should be through the inherent flexibility of this AT-rich region. Secondly, a set of sequence-specific bonds between protein side chains and bases in the major groove arise in the region -11 to -7. In this case, the recognition is achieved via the formation of hydrogen bonds with the appropriate acceptor or donor chemical groups in the base-pairs sides (See Fig. 1 and Fig. 2). Finally, the polymerase opens the region from -4 to -1 relatively to the starting site of transcription, by inserting a  $\beta$ -hairpin and binding the melted template strand.

Among the three polymerase-promoter interactions mentioned above, the third one involves a strand separation which arises only after the promoter recognition, and is for this reason most specific to the open complex formation. We will therefore make the assumption that it does not interfere directly in the promoter search. The other two interactions are both possible candidates for a recognition mechanism. Here we focus on the hydrogen bond mediated interaction, that has the strongest sensitivity to the basepairs, and we address the question if a specific interaction of this type can represent the main reading tool which influences the polymerase motion. To this regard we remark that the hydrogen bond acceptors and donors are regularly positioned on the promoter major groove: the DNA geometry is in fact such that each of the four different basepairs exposes four possible major groove interacting sites as depicted in Fig. 1 (Seeman *et al.*, 1976). These sites can be either H-bond acceptors and donors, or sites where a hydrogen atom or a methyl group are present. In the latter cases they do not bond directly to polymerase (at least at the promoter site). In Fig. 2 the H-bonds actually made between polymerase and DNA at the promoter, as revealed by the crystallographic analysis, are reported. The two semicircles in the left part of Fig. 2 and their correspondent positions on the right pattern, refer to the presence of a hy-

<sup>1</sup>See Figs. 1 and 2 in Ref. (Cheetham *et al.*, 1999) for a clear representation of the whole set of interactions.

drogen bond which is shared between two DNA sites through a water molecule (Cheetam *et al.*, 1999).

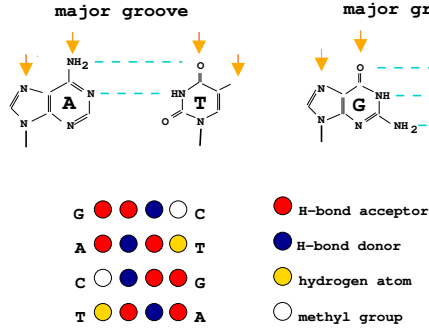


Figure 1: The positions of all the possible major groove interacting sites where base-pairs can make hydrogen bonds (*top*) and the corresponding chemical groups (*bottom*). Blue and red disks indicates the hydrogen donor and acceptor DNA groups respectively. White positions correspond to hydrogen atoms and yellow ones to methyl groups. Each basepair is associated with a different  $1 \times 4$  pattern.

We shall assume that, in each position along DNA, the RNAP “tries” to make the same set of hydrogen bonds which corresponds to the promoter, testing in this way the underlying sequence. It is convenient to represent the RNAP by a recognition matrix able to match its target sequence, i.e. containing the pattern of chemical active groups that allows the best binding at the promoter. We suppose therefore that each position along DNA will have a certain number of made (*matches*) and unmade (*mismatches*) hydrogen bonds with the polymerase recognition matrix. For simplicity, we will represent the recognition pattern directly in terms of its corresponding binding sites on DNA <sup>2</sup>.

One expects that each match will stabilize the complex, while mismatches will act as to destabilize RNAP, that will tend therefore to move away from the “wrong” positions (von Hippel and Berg, 1989; von Hippel *et al.*, 1996). For each position  $n$  along the chain we define an energy  $E(n)$ , simply by counting the number of matches and mismatches, and adding a corre-

<sup>2</sup>This is also a way to remind that we actually do not include in the model all the possible polymerase-DNA nonspecific bounds, but only those that are made at the promoter, for which an experimental evidence is available.

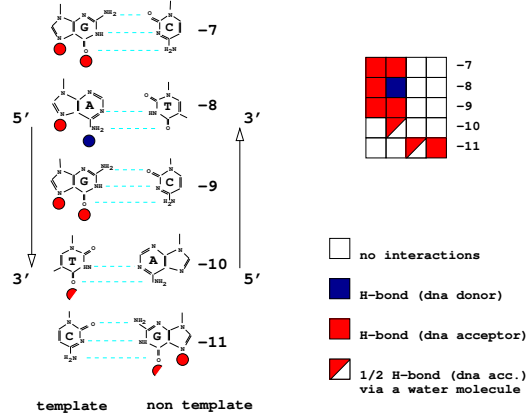


Figure 2: A sketch of the DNA interaction sites at the promoter, where hydrogen bonds with corresponding RNAP chemical groups are made. Blue and red disks indicate the hydrogen donor and acceptor DNA groups respectively; the two half disks correspond to a couple of sites that could share a water mediated hydrogen bond. On the right, the corresponding  $5 \times 4$  pattern that RNAP recognizes.

sponding negative or positive amount of energy, respectively (empty sites in the recognition matrix do not contribute to the energy). Polymerase interacting sites corresponding to the semicircles in Fig. 2 are evaluated in a first approximation as half hydrogen bonds everywhere along the chain.

Formally, the energy is defined by denoting by  $+1, -1, 0$  respectively the acceptor, donor, and non interacting DNA sites. The DNA sequence is then represented as a list of vectors,  $\dots b_{n-1}, b_n, b_{n+1}, \dots$ , where

$$b_n = \begin{cases} (1, -1, 1, 0)^T & \text{for base A} \\ (0, 1, -1, 1)^T & \text{for base T} \\ (1, 1, -1, 0)^T & \text{for base G} \\ (0, -1, 1, 1)^T & \text{for base C} \end{cases}$$

The polymerase then acts at a position  $n$  on the sequence of 5 bases which we represent by the  $4 \times 5$  matrix  $D_n = (b_n, b_{n+1}, b_{n+2}, b_{n+3}, b_{n+4})$ . The consensus sequence GAGTC at the promoter site corresponds therefore to the matrix

$$D_n = \begin{pmatrix} 1 & 1 & 1 & 0 & 0 \\ 1 & -1 & 1 & 1 & -1 \\ -1 & 1 & -1 & -1 & 1 \\ 0 & 0 & 0 & 1 & 1 \end{pmatrix}.$$

We then define a  $4 \times 5$  recognition matrix

$R(i, j)$ , corresponding to Fig. 2,

$$R = \begin{pmatrix} 1 & 1 & 0 & 0 \\ 1 & -1 & 0 & 0 \\ 1 & 1 & 0 & 0 \\ 0 & 1/2 & 0 & 0 \\ 0 & 0 & 1/2 & 1 \end{pmatrix}$$

where the factors 1/2 have been introduced in order to reproduce the shared hydrogen bond, previously mentioned. With this notation, the interaction energy can be written simply as

$$E(n) = -\mathcal{E} \operatorname{tr}(R \cdot D_n) \quad (1)$$

where the dot  $\cdot$  denotes the usual matrix multiplication and  $\operatorname{tr}$  is the trace. Minima correspond to the complete matching and thus to the recognition sequence GAGTC. Each positive or negative contribution to the energy,  $\mathcal{E}$ , is equal to a hydrogen bond energy. Note that the mobility of RNAPs dramatically depends on  $\beta\mathcal{E}$ . At room temperature,  $k_B T$  is about 0.025 eV (or  $RT = 0.6$  kcal/mol,  $R = N_a k_B$ ); the energy barriers must be smaller in order to allow the RNAP to move and reach the promoter site<sup>3</sup>. Since there are no direct measurements of the interaction energies during sliding and it is difficult to make an estimate of the involved hydrogen bond strength, we shall use  $\beta\mathcal{E}$  as a free parameter. The resulting energy  $E(n)$  defines an irregular landscape on which the polymerase can move as it will be discussed in the next subsection.

## 1.2 Sequence dependent RNAP diffusive model

We shall introduce in this subsection four versions of the model corresponding to different mechanisms allowing the fundamental translocation step in the enzyme motion. The length of hydrogen bonds (up to 3.5 Å in DNA-protein interactions (Nadassy *et al.*, 1999)) can roughly reach the same order of magnitude of the distance between base pairs (3.4 Å). So the RNAP may eventually shift directly from one position to the next one without activation energy for the one step process. If, on the contrary, the

<sup>3</sup> This may seem not consistent with the usual measured strength of chemical hydrogen bonds, which normally corresponds to a few kcal/mol (Stryer, 1995; Voet and Voet, 1995). The strength of one hydrogen bond is, however, very sensitive to distance and orientation, so that the relative position of the DNA and the reading RNAP may be responsible of a relevant lowering of the interaction energy.

RNAP has to partially or completely disrupt all hydrogen bonds on one site before moving to the next position, we need to consider the possibility that the translocation has an additional activation barrier.

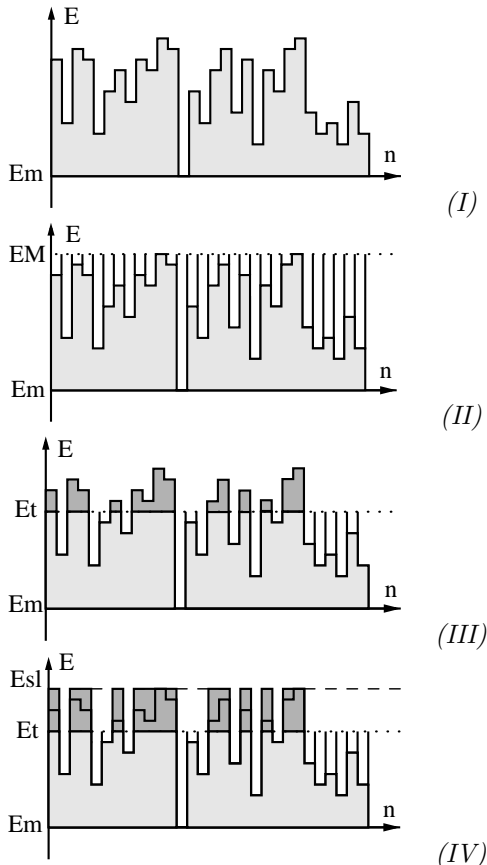


Figure 3: The four considered variants of the model.

Furthermore, RNAP could have some internal flexibility allowing conformational changes, eventually depending on the local degree of stability: i.e., it is possible that, if too many mismatches are found, RNAP should undergo a conformational change from a "reading" mode to a "sliding" mode, where no hydrogen bonds are effectively made (von Hippel *et al.*, 1996). In this case, one has a sort of two-states model, for which, if the total energy  $E(n)$  is over a threshold  $E_t$ , the system passes to a different state of constant energy  $E_{sl}$  where RNAP can freely slide.

In order to have a first insight over all these possibilities, we define and analyze some different models, sketched in Fig. 3 and listed here-

after:

- I) *no threshold model*: hydrogen bonds can directly translate from one position to another without being destroyed. In this case the energy difference from  $n$  to  $n' = n \pm 1$   $\Delta E(n \rightarrow n')$  is simply

$$\Delta E(n \rightarrow n') = \max[E(n') - E(n), 0]; \quad (2)$$

here  $\Delta E(n \rightarrow n')$  is set to zero if  $E(n') - E(n)$  is negative, as usual.

- II) *maximal threshold model*: in order to reach a next site, RNAP must destroy all bonds and pass through a state of "total mismatch". In this case  $\Delta E(n \rightarrow n') = E_M - E(n)$ , where  $E_M = \max[E(n)]$ .
- III) *intermediate threshold model*: in order to reach a next site, RNAP must pass through an intermediate "zero" state defined by a threshold energy  $E_t$ . One has therefore

$$\Delta E(n \rightarrow n') = \max[E_t - E(n), E(n') - E(n), 0]. \quad (3)$$

Models *I* and *III* are actually the two limiting cases of model *III* when the threshold is set to the minimum and maximum values of the potential energy, respectively. These three models could therefore be considered as three cases of an *unique model*, just dependent on the choice of the energy threshold. We will anyway refer to these three cases as to models *I*, *II* and *III* in the following, for aim of readability. Note that in the general case of an intermediate threshold, the previous model gives two different possible regimes for the polymerase, because the energy profile features change for regions where  $E(n)$  is greater or lower than  $E_t$ . On the basis of the previous consideration, we also want to include in our analysis a stronger separation between sites of low or high matching. As mentioned, we assume indeed that an additional conformational change unable RNAP to make hydrogen bonds in the less favorable regions. We will define therefore a fourth model as follows:

- IV) *two-regimes model*: a threshold energy  $E_t$  separates "reading" regions, where the energy is  $E(n) < E_t$  from "sliding" regions, where no hydrogen bonds are made and the RNA polymerase can freely diffuse on a flat energy landscape,  $E(n) = E_{sl}$ . Below the threshold, the barrier  $E_t$  still affect

the translocation as in case of model *III*. For simplicity, we will fix the value of  $E_{sl}$  to  $E_M = \max[E(n)]$ . In this case, one can redefine the energy as

$$E(n) = \begin{cases} E(n) & \text{if } E(n) < E_t \\ E_{sl} & \text{if } E(n) \geq E_t \end{cases} \quad (4)$$

and the translocation barrier results to be defined as in case *III*.

Note that our model *IV* interpolates between straight sequence-dependent walk (model *I*) and the biological model of the promoter search proposed by von Hippel in Ref. (von Hippel and Berg, 1989; von Hippel *et al.*, 1996). The scenario suggested by von Hippel relies indeed on the idea that the specific interaction, given essentially by the same hydrogen bond pattern considered here, is "switch off" by a conformational change if too many mismatches are present. RNAP is in this picture more often in a "sliding" mode, where the specific hydrogen bond interactions are inactive. A quantitative description of this mechanism can be obtained by the introduction of our model *IV*, where the varying threshold level  $E_{sl}$  accounts for the degree of homology which leads to the supposed RNAP conformational change.

The rates  $r_{n \rightarrow n'}$  of translocation between neighboring sites  $n$  and  $n'$  are, according to the *Arrhenius law*, proportional to  $\exp(-\beta \Delta E(n \rightarrow n'))$ , where  $n' = n \pm 1$ . The model includes a nonzero probability for the polymerase to stop at one position; the complete set of translocation rates reads therefore:

$$\begin{cases} r_{n \rightarrow n'} &= 1/2 \exp(-\beta \Delta E(n \rightarrow n')), \\ & n' = n \pm 1 \\ r_{n \rightarrow n} &= 1 - r_{n \rightarrow n+1} - r_{n \rightarrow n-1}. \end{cases} \quad (5)$$

Note that the case  $r_{n \rightarrow n'} = 1/2$  corresponds to  $\Delta E(n \rightarrow n') = 0$ . This case is therefore equivalent to the case of a (locally) constant energy landscape, i.e. to a simple one-dimensional diffusion process with diffusion constant  $D = 1/2$ <sup>4</sup>.

Let us now consider the distribution of energy levels that is obtained when the real T7 DNA sequence (?) is considered and the energy landscape is evaluated through the local

<sup>4</sup>If the distance  $\ell = .34 \text{ nm}$  between basepairs in DNA and a discretization of time  $t = \eta m$  are taken into account, a factor  $\eta \ell^2$  must be included into the definition of  $D$ .

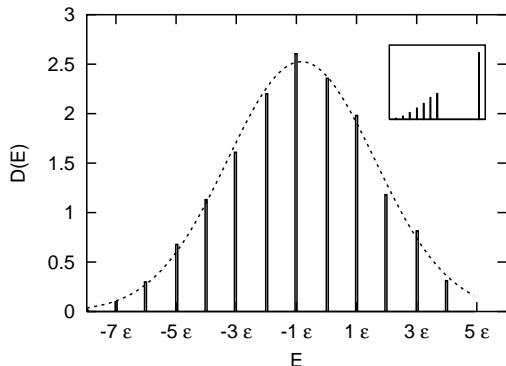


Figure 4: Energy level distribution (models I to III). A Gaussian fit (*dashed line*) is superimposed for comparison. *Inset*: The same distribution for model IV ( $E_t = 0$ ).

degree of homology by Equation (1). In Fig. 4 the energy distribution evaluated on the whole T7 sequence is represented. As it can be seen by comparing with the superimposed fit, the resulting distribution is, for models I to III, almost Gaussian. Note that in the case of model IV all contributions to levels above the threshold  $E_t$  are obviously condensed in a unique level  $E_{sl}$  (see *Inset*). The Gaussian distribution does not indicate by itself which correlation properties characterize the energy  $E(n)$ . In order to have insights on the correlation in the energy landscape, we have therefore analyzed its correlation function and its spectrum, and compared with the corresponding functions obtained by using an artificial random DNA sequence. Roughly speaking, the correlation function in both cases is approximatively zero after 1 step. Nevertheless, some correlations, known to be present in T7 DNA, namely the three-periodicity associated with the genetic code, results to be reflected in the distributions of H-bond interaction energies considered in our model.

## 2 Results: recognition efficiency and anomalous diffusion

The first important check of the four RNAP models is related to their capability of finding the promoter region. Theoretically, one can easily estimate the stationary distribution of a population of polymerase on the four different

model landscapes as

$$\rho_\infty(n) \propto e^{-\beta E(n)} \quad (6)$$

As usual, the stationary distribution only depends on the site energy, and not on differences and thresholds. As a consequence, models I to III have the same distribution, whereas the redefinition of energy in model IV leads to a substantially different result. Equation (6) straightforwardly implies that the recognition sites, which have the lower energy, will be in average the most populated.

In order to verify that this is indeed obtained in a dynamical context, we simulated numerically the time evolution of models I to IV taking as initial condition an uniform distribution of independent RNAPs on a DNA region of 1000 base-pairs, with 30 polymerases per site. Note that the assumption of an uniform initial distribution of a set of polymerases corresponds, statistically, to consider the probability evolution of a single polymerase binding to DNA at random site. The simulation is performed on the first 3000 base-pairs region of the T7 sequence, which contains two recognition sequences GAGTC, at positions 1126 and 1435. We used here  $\beta\mathcal{E} = 0.5$ .

After a sufficiently long time, the polymerase distribution  $\rho(n)$  spreads out, as shown in the inset of Fig. 5, and shows a series of peaks corresponding to the sites with larger occupancy. Where the border effects can be neglected, this distribution tends to its equilibrium limit; this is shown in Fig. 5, where we plot a portion of the distribution obtained after  $10^6$  time steps for model I, together with  $\rho_\infty$ . As expected, the larger peaks correspond to energy minima, i.e. to the location of the two recognition sequences GAGTC present in this DNA region. For all the models I to III the final distribution is similar, with the two highest peaks exactly in correspondence to the two recognition sequences, this confirming that the energy landscape defined on the basis of the pattern matching actually tends to guide polymerases to the promoter recognition sequences.

Note that, in case of model IV, the distribution of levels is different, this obviously implying a different shape for  $\rho_\infty(n)$ . The case of a sufficiently low threshold energy is reflected on an asymptotic distribution with rarer, larger picks on a very low constant underground (data not shown).

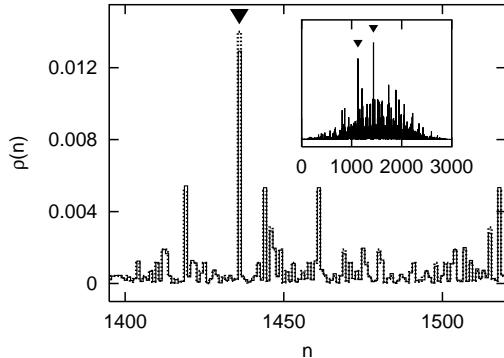


Figure 5: A central portion of the polymerase distributions  $\rho(n)$  for model *I* after an integration time of  $10^6$  integration steps, obtained by averaging over  $3 \cdot 10^4$  particles initially uniformly distributed in the interval  $[1000, 2000]$  (solid line). The analytical equilibrium distribution  $\rho_\infty(n)$ , (dotted line) is shown for comparison.  $\beta\mathcal{E} = 0.5$ . *Inset*: the whole distribution at the same time. In both plots, the arrows indicate the location of the recognition sequences GAGTC (sites 1126 and 1435).

We now investigate the dynamical behavior of the four models, and check if there are some relevant deviations from random walk, induced by the sequence sensitivity. For large values of  $\beta\mathcal{E}$  some positions along DNA could trap polymerases for long times, this implying that, at small and intermediate times, the diffusion could be substantially different than for a pure random walk. In order to estimate this effect, we calculate the mean square deviation from the average of the spatial displacement,

$$\langle \Delta n^2 \rangle = \langle \Delta n^2(t) \rangle = \sum_{i=1}^N (n_i(t) - n_i(0))^2. \quad (7)$$

The average is made, at fixed time, on  $N = 9 \cdot 10^3$  particles, initially distributed uniformly in the DNA region  $[1000, 2000]$ . This procedure therefore includes both an ensemble average on a large number of particles and average on a large set of initial conditions.

Starting from model *I*, we investigate the dependence on  $\beta\mathcal{E}$  of the diffusive behavior. Results are reported in Fig. 6.

In the limit of a  $\beta\mathcal{E} = 0$ , i.e. in the case of a flat underlying potential (or  $T = \infty$ ), the diffusion is of course standard, with  $D = 1/2$  and a linear dependence on time, so that the cor-

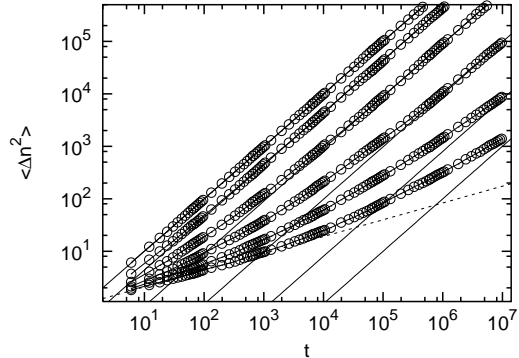


Figure 6: Diffusion behavior of model *I* for different values of  $\beta\mathcal{E}$ . From the upper curve to the bottom:  $\beta\mathcal{E} = 0, 0.3, 0.6, 0.9, 1.2, 1.5$ . Note the log-log scale: a linear diffusion  $\langle \Delta n^2 \rangle \propto t$  corresponds in this graph to the straight lines of unit slope (solid lines), while slopes lower than 1 correspond to  $\langle \Delta n^2 \rangle = A t^b$ , with  $b < 1$ . A (dashed) line of slope 0.3 is reported for comparison.

responding curve is a straight line of slope 1 in the log-log plot. For larger values of  $\beta\mathcal{E}$  (smaller temperatures compared with the energy fluctuations), the dynamics of the model shows initially large deviations from the normal diffusion: in these finite temperature cases, the motion is initially subdiffusive, with

$$\langle \Delta n^2 \rangle = A t^b, \quad b < 1. \quad (8)$$

The exponent  $b$  increases then with time toward its equilibrium value of 1. The initial deviation  $(1 - b)$  and the time needed to reach the limit  $b = 1$  both increase with  $\beta\mathcal{E}$ . This behavior does not depend on the choice of the initial conditions and it is not a transient induced by some  $t = 0$  properties: we have verified indeed that qualitatively the same time dependence is reproduced after an initial transient time of  $10^4$ ,  $10^5$  or  $10^6$  time steps. As expected, once reached the normal diffusion regime, different temperatures correspond to different diffusion constants  $D$  (in the log-log representation,  $2D$  corresponds to the offset of the lines of slope 1, according to the relation  $\log \langle \Delta n^2 \rangle = \log 2D + \log t$ ).

As we will discuss later, the possibility to observe, at small and intermediate times, an anomalous diffusion, can be helpful in the comparison with experiments and, therefore, in the fit of the model parameters.

We will now extend the diffusion analysis to the other versions of the model, introduced in Section 1. Resulting curves for models *I* to *IV* and for  $\beta\mathcal{E} = 1$  are reported in Fig. 7. We use here  $E_t = 0$ , in models *III* and *IV*, as an intermediate value, corresponding to the condition of a complete balance between matches and mismatches.

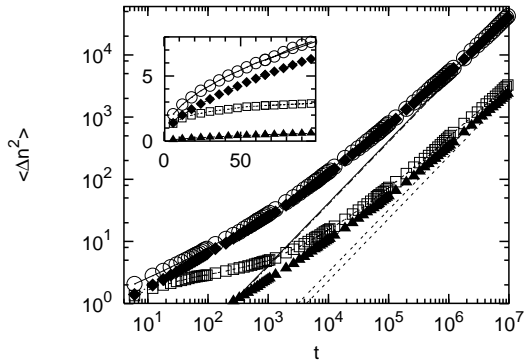


Figure 7: Mean square deviation  $\langle \Delta n^2 \rangle$  for the four different models, with  $\beta\mathcal{E} = 1$  and  $E_t = 0$ , in the log-log representation. Symbols refer respectively to: open circles, model *I*; triangles, model *II*; diamonds, model *III*; squares, model *IV* ( $E_t = 0$ ). The straight lines correspond to the fit in the last part of the graphs ( $t \in [6 \cdot 10^6, 10^7]$ ). *Inset*: the same curves in a linear representation in the short time regime (symbols have the same meaning).

As for model *I*, we observe in all cases a *short time regime* where the diffusion displays anomalous, subdiffusive features. The initial values of the exponent  $b$  have been fitted in the time range  $(0, 100)$  through the function  $At^b$  and result to be as follows for the first three models:

$$\begin{aligned} I : b &= 0.49 \pm 1\% \\ II : b &= 0.61 \pm 1\% \\ III : b &= 0.56 \pm 1\%. \end{aligned}$$

Note that model *IV* displays in this short time regime a particular behavior, that will be discussed in the following. The previous results clearly display that a strong anomalous diffusion characterizes the initial time, due to the trapping effect of the rough energy landscape.

In principle, the anomalous diffusion observed in our models could be due to some particular spatial correlation properties of the underlying

potential. Nevertheless, we have checked that it is only due to the roughness of the landscape, doing the same experiment on an artificial base sequence, completely random. In the conditions described by model *I*, for instance, and in the same fit range, we obtained  $b = 0.52 \pm 1\%$ , and a curve that displays good agreement with the T7 DNA case (data not shown).

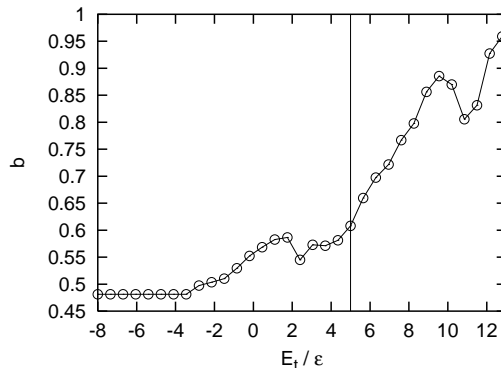


Figure 8: Behavior of the exponent  $b$  as fitted in the short time regime  $t \in (0, 100)$  as a function of the threshold energy  $E_t$  for model *III*. The vertical line corresponds to  $\max[E(n)] = 5\mathcal{E}$ .

For model *III* with varying threshold (i.e., including model *I* and *II*) it is interesting to study the behavior of the short time subdiffusive exponent  $b$  as a function of  $E_t$ . Such analysis is reported in Fig. 8. For thresholds lower than a critical value of about  $-3$ , the system displays almost no sensitivity to the threshold level. This is due to the fact that, in order to have some relevant effect, it is necessary to have not only a site  $n$  with  $E(n) < E_t$ , but also at least one of its two neighboring sites should be below the threshold. The probability of finding two adjacent sites below the threshold is too low below for  $E_t \leq -3$ , this explaining the previous result. Interestingly, the exponent  $b$  becomes a nonmonotonic and very sensitive function of  $E_t$  for larger values of  $E_t$ . The effect of the threshold in this intermediate regime is in fact twofold: from one side, it induces an additional damping on many low energy sites, from the other, it makes (a fraction of) these same sites “blind” to the energies of their neighborings (the translocation barriers only will depend on  $E(n)$  and  $E_t$ ). The complex balance between the two contributions induces the high instability of the fit results displayed in Fig. 8. As the threshold in-

creases above the maximum level ( $E_t = 5$ ), the disorder of the underlying energy landscape becomes less and less important, and the system tends to recover a standard diffusive behavior strongly damped, i.e. with  $b \rightarrow 1$  and  $A(D) \rightarrow 0$  (the behavior of  $A$  is not shown in Fig. 8; for  $E_t > 12\mathcal{E}$  the dynamics becomes so slow that it becomes impossible to fit  $\langle \Delta n^2 \rangle$  with our simulation conditions).

The asymptotic (standard) diffusion constant depends on the model choice. A linear fit of the *large time regime* of  $\langle \Delta n^2 \rangle$  of Fig. 7 has been done in order to have an estimate of the average diffusion constant  $D$ , in the random walk approximation where  $\langle \Delta n^2 \rangle = 2Dt$ . Besides, we checked that an effective linear behavior is reached in the corresponding time range by fitting again with a function  $\langle \Delta n^2 \rangle = At^b$  and verifying that  $b$  is close to unity.

The standard diffusion limit is better achieved for models displaying a faster diffusion. The resulting diffusion constants  $D$  and the scaling exponents  $b$  for the four models in the large time regime ( $t \in [6 \cdot 10^6, 10^7]$ ) are given, for  $E_t = 0$ , respectively by:

$$\begin{aligned} I : \quad 2D &= 4.1 \cdot 10^{-3} \pm 1\% & b &= 0.93 \pm 1\% \\ II : \quad 2D &= .23 \cdot 10^{-3} \pm 2\% & b &= 0.86 \pm 1\% \\ III : \quad 2D &= 4.0 \cdot 10^{-3} \pm 1\% & b &= 0.91 \pm 1\% \\ IV : \quad 2D &= .32 \cdot 10^{-3} \pm 1\% & b &= 0.85 \pm 1\% \end{aligned}$$

The corresponding curves are reported by straight lines in Fig. 7.

The differences in the equilibrium diffusion constant between different models are easily related to the effect of the activation barrier in the four cases: the highest is the threshold energy to overcome in order to move of one step, the lower is the diffusion. Note that in the case of model *IV* the boundaries between flat and original potential regions act as energy barriers of amplitude  $\approx E_{sl}$ : these barriers appear to affect the motion more strongly than the threshold  $E_t$ , this resulting in a diffusion constant closer to that of model *II* than to model *III*.

As done for the parameter  $b$  in the short time regime, we can analyze the dependence of the asymptotic diffusion parameter  $2D$  on  $E_t$ . Fig. 9 shows indeed the behavior of the standard diffusion parameter for different values of  $E_t$  (model *III*). For technical reasons, we display data resulting from the fit in the range  $(8 \cdot 10^5, 10^6)$ , i.e. in a region where the parameter  $b$  has not yet reached unity. The curve of Fig. 9 represents

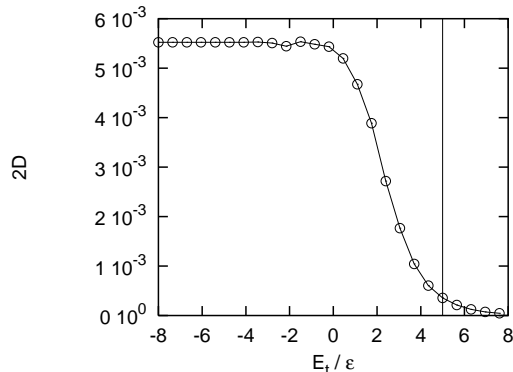


Figure 9: Behavior of the coefficient  $2D$  as fitted in the large time regime  $t \in (8 \cdot 10^5, 10^6)$  as a function of the threshold energy  $E_t$  for model *III*. The level  $\max[E(n)] = 5\mathcal{E}$  is represented by a vertical line.

therefore only a qualitative analysis and shows some small discrepancy with data given in Eq. 9. Again, almost no sensitivity to the threshold level is observed below a critical value, approximately  $E_t = -3$ . Roughly between this value and  $E_t = 0$ , we observe a transition to a regime of strong sensitivity ( $E_t > 0$ ), where the damping effect induced by the threshold is much more enhanced. The diffusion constant tends to vanish just above the maximal energy ( $E_M = 5$ , vertical line), as intuitively expected, and in accordance to what happens for the short time regime.

We shall now discuss in more details model *IV*, since it displays, with respect to the others, a more complicated behavior. Note that, in principle, model *IV* can be put exactly in the same scheme of other models, once redefined the underlined potential  $E(n)$  according to Equation (4). Nevertheless, this redefinition of the energy landscape leads to substantial different features. As it can be observed in Fig. 10, during an initial time laps the model diffuse more rapidly, even if still subdiffusively, with initially a larger instantaneous diffusion constant. The initial speeding up of the dynamics is more important as the value of the threshold decreases, i.e. as the energy redefinition involves an increasing number of sites. This effect can be explained by considering how the potential landscape is changed for model *IV*. Among the particles, uniformly distributed at time zero over a large region of the sequence, all those that are initially on flat regions of energy  $E_{sl}$  will start

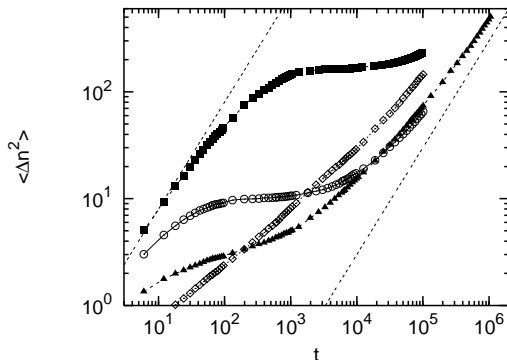


Figure 10: Time behavior of  $\langle \Delta n^2 \rangle$  for model IV, in the cases  $E_t = -4$  (full squares),  $E_t = -2$  (circles),  $E_t = 0$  (full triangles),  $E_t = 2$  (diamonds), and with  $\beta\mathcal{E} = 1$ . Two straight lines of slope 1 are shown for comparison.

diffusing freely with diffusion constant equal to  $1/2$ , until they fall down in one  $E < E_t$  region. These particles contribute initially to the diffusion with a large term, thus making it increase. After an initial transient, however, most of the particles will be almost trapped in the potential wells, and a stationary distribution of the particles will be reached, with a corresponding stationary diffusion behavior.

More precisely, the trapping effect will depend on the value of  $E_{sl}$ , set to  $\max[E(n)]$  in our calculations. If  $E_{sl}$  is big enough, most of the particles will be trapped in  $E(n) < E_t$  regions, with activation barriers and only a small probability to escape again toward the flat plateaux. Therefore, in the long time regime, the system will be essentially in the same state model III, but mostly localized in some finite regions. Note that, if the trapping were perfect, the limiting diffusion constant would be zero: for finite, but large enough  $E_{sl}$ , there is a probability for particle to explore the whole space by overcoming a boundary barrier, and therefore a nonzero diffusion constant. In other words, the particular equilibrium conditions introduced in model IV are indeed such that one particle needs to spend a large amount of energy (and, therefore, of time) before reaching a high level plateau, but once reached, it can move much faster to the next favorable site.

An analytical derivation of the main dynamical quantities as functions of the model parameters discussed in this section will be presented

in a forthcoming paper (Barbi *et al.*, 2002).

### 3 Discussion

All the results presented in this work can be checked by a comparison with detailed experimental results. As mentioned in the Introduction, experiments leading to a rather precise determination of the RNAP position along DNA at different times during the promoter search have already appeared (Kabata *et al.*, 1993; Harada *et al.*, 1999; Guthold *et al.*, 1999), and others are in preparation (Place *et al.*, 2001). This will give for the first time the possibility to estimate the detailed features of the polymerase diffusive motion. As we have shown, a dynamical model which include the affinity for the promoter together with the possibility of sliding, leads to a nontrivial sequence dependent dynamics, at least in some range of the parameters.

The mean sliding distance is kinetically evaluated in different experiments around 350 – 1000 bps ((Shimamoto, 1999) and references herein). This is probably not peculiar to RNAP since other enzymes interacting with DNA seems to slide along the DNA for a short distance before being released in solution (Stanford *et al.*, 2000). In this regime, the anomalous diffusion behavior is predominant for our model. In particular, the recent scanning force microscope (SFM) experiment, performed by Guthold *et al.* (Guthold *et al.*, 1999), allows a direct observation of single RNAPs sliding back and forth on a single DNA chain partially adsorbed on a mica surface, although with some technical limitations (the average lifetime of the nonspecific complex is more than hundred times larger than what measured in solution, probably due to the two-dimensional constraints). In Ref. (Guthold *et al.*, 1999), the statistical properties of the observed diffusive motion have been fitted by the law  $\langle \Delta x^2 \rangle \simeq 2Dt$ , in order to confirm the general assumption that RNAP moves randomly along DNA. Quantitatively, however, in the observed displacement ranges (less than two hundreds basepairs), the fit seems to deviate from a pure diffusive motion. This is perhaps due to the experimental constraints and to the limited number of RNAP sliding trajectories (about 30) used in the experiment. Therefore, this observation suggests that a re-examination of these direct AFM sliding measurements could be of

extreme interest. We have tried to extrapolate the numerical data from Fig. 2 of Ref. (Guthold *et al.*, 1999) and to fit the resulting  $\langle \Delta n^2 \rangle$  with a power law of the type  $At^b$ . This rough estimate gives  $b \sim 0.5 \pm 15\%$ . Even if in this experiment the polymerase motion is probably slowed down by some technical constraints, it is very interesting to notice that the corresponding data seem much better compatible with a subdiffusive behavior than to normal diffusion, as usually assumed. This first experiment allowing a direct visualization of the RNAP sliding motion seems to give therefore, from our point of view, some intriguing and encouraging results.

We remark that the dynamical features described here depend crucially on the choice of the model parameters: the ratio  $\beta\mathcal{E}$  between the typical bond energy  $\mathcal{E}$  and the thermal energy  $k_B T$ , the value of the energy threshold  $E_t$ , and, in the case of model *IV*, the energy of the plateaux  $E_{sl}$ . Further experimental investigations, devoted to the detailed determination of the nonspecific interactions, are therefore necessary to improve the model. The version of the model resulting compatible with the sliding RNAP dynamics of single molecule experiments should emerge from comparisons with the experimental data, using the model parameters as fitting parameters. In practice, the complicated diffusive behavior of the model will allow us to compare theory and experiments by means of more than one dynamical observable. For the case of model *IV*, where the additional model parameter  $E_{sl}$  is needed, the presence of a new short-time specific feature could be used in the fit of the experimental results.

From a biological point of view, the four models offer a framework for defining the pertinent parameters to optimize the promoter search. For all models, the specific interaction energy between RNAP and DNA is crucial and should be close to  $k_B T$  in order to allow the polymerase motion. This adjustment of the interaction energy can be achieved by varying the distance and angle of the H-bonds during sliding. Different DNA interacting proteins should have developed different energy landscapes associated with this interaction. The  $E_t$  threshold, the activation state to pass from one position to the next one, and the  $\beta\mathcal{E}$  parameter, both have a strong effect on the subdiffusive behavior of the protein at the beginning of the DNA-protein interaction. But perhaps, the more interesting model from a biological point of view is model *IV*, since it

allows a more important control of the diffusion pattern. An exact balance has to be found in biological system between the reading and sliding mode.  $E_t$ ,  $E_{sl}$ , and  $\beta\mathcal{E}$  have to be optimized for the biological purpose which will be physically reflected by the protein-DNA interaction and by the DNA sequence. Varying the diffusion pattern will offer more checkpoint in the control of transcription initiation.

Finally, it is important to stress that the recognition mechanism through hydrogen bonds considered here does not allow a complete identification of the promoters. The occurrences of the recognition sequence GACTC, or of the complementary sequence GAGTC in the T7 genome are in fact more than 90; among them only 10 are nevertheless appropriately combined to weak (AT-rich) sequences in longer promoter-like sequences of the type [weak]<sub>5</sub>-X-GACTC. Evidently, other "signals" must cooperate with the direct pattern recognition mechanism in order to allow the polymerase find its target. A sensitivity to the minor groove flexibility is a good candidate as an additional recognition tool, also in consideration of similar results obtained e.g. for the case of reverse transcriptase (Lavigne and Buc, 1999). In this sense the presented model represents a first attempt toward a detailed description of the RNAP dynamics during the promoter search. It can be improved by including more details about the RNAP-DNA interaction as they became available from new experimental results. We believe, however, that the main idea of the model, which is the link between base sequence and dynamics, will remain true in general. Indeed, as far as a sequence dependence is considered, the enzyme will always interact through an effective energy with a pseudo-random fluctuating profile. The resulting roughness can be generated by different kind of interactions, but is in principle sufficient to obtain anomalous diffusion features as those described in this paper.

## Conclusions

In this paper we have proposed a simple model for the RNAP sliding motion along DNA, which include a sequence dependent interaction. The nature of the actual interaction being poorly known, we deduced an hypothetical polymerase-DNA interaction from the crystallographic structure of the T7 polymerase-

promoter complex (Cheetam *et al.*, 1999). We have included four possible variations by considering slightly different translocation probabilities, i.e. by the presence of a variable activation barrier  $E_t$  (leading to models *I* to *III*), and eventually by distinguishing “reading” regions from “sliding” regions, where no hydrogen bonds are made so that the RNAP can freely diffuse at an effective constant energy (model *IV*).

The four versions of the model all lead to a certain efficiency in the promoter recognition, which is essentially limited by the trapping in sites with a minor degree of homology. A numerical study of the diffusion properties of the model shows that a normal diffusion regime is only achieved after an initial characteristic time. We have shown as all the four models are characterized at shorter times by a subdiffusive regime. This result is of particular interest because, as we have discussed, the anomalous diffusion is observed in a range that corresponds approximately to the range of the experimental mean distance covered by the RNAP during sliding (Shimamoto, 1999). This particular behavior can be easily compared with experiments, so that the model parameters can be used as fitting parameters. We have analyzed the details of the diffusion in the different regimes and for the different models. Finally, we have described the very short time behavior of the *two-regimes* model, which displays richer features. The physical reasons underlying the different diffusion behaviors have been discussed.

The ability of constraining and manipulating biological object represent actually the main power of the sophisticated and exciting results obtained at present days by nano-technologies and single molecule experiments. The present paper represents a first step toward a theoretical picture where the new experimental results could be correctly analyzed and connected with the known functional properties of the corresponding biological systems. In this respect, it is also important to keep in mind that the *in vivo* dynamics of the corresponding biological processes occur in a high density environment, characterized by very complex spatial structures and mainly bound and structured water (Goodsell, 1992). What we usually call the diffusive motion of proteins inside the cell, is likely to be instead a motion strongly dependent on a complex set of environmental trapping sites, as in the case considered here. In this respect, the approach proposed in this paper may have a larger

range of application.

We are grateful to A. Lesne, M. Peyrard and S. Ruffo for helpful discussions. M.B. wishes to thanks the EU and the Physics Department of the University of Salerno, Italy, for a two years post-doctoral research grant during which this work was done. V.P. acknowledges the Physics Department of the University of Salerno for financial support of two short term visits during which part of this work was done. M.S. acknowledges partial support from MURST through a PRIN-2000 Initiative and from the European grant LOCNET n.o HPRN-CT-1999-00163.

## References

- Barbi, M., V. Popkov, and M. Salerno, 2002, in preparation.
- Cheetam, G. T., D. Jeruzalemi, and T. A. Steitz, 1999, *Structural basis for initiation of transcription from an RNA polymerase-promoter complex*, Nature **399**, 80.
- Goodsell, D. S., 1992, *A look inside the living cell*, Amer. Scientist **80**, 457.
- Guthold, M. *et al.*, 1994, *Following the assembly of RNA polymerase-DNA complexes in aqueous solutions with the scanning force microscope*, Proc. Natl. Acad. Sci. U.S.A. **91**, 12927.
- Guthold, M. *et al.*, 1999, *Direct observation of one-dimensional diffusion and transcription by escherichia coli RNA polymerase*, Biophys. J. **77**, 2284.
- Harada, Y. *et al.*, 1999, *Single-molecule imaging of RNA polymerase-DNA interactions in real time*, Biophys. J. **76**, 709.
- von Hippel, P. H. and O. G. Berg, 1989, *Facilitated Target Location in Biological Systems*, J. Biol. Chem. **264**, 675.
- von Hippel, P. H. *et al.*, 1996, *Specificity mechanisms in the control of transcription*, Biophys. Chem. **59**, 231.
- Kabata, H. *et al.*, 1993, *Visualisation of single molecules of RNA polymerase sliding along DNA*, Science **262**, 1561.

- Lavigne, M. and H. Buc, 1999, *Compression of the DNA minor groove is responsible for termination of DNA synthesis by hiv-1 reverse transcriptase*, J. Mol. Biol. **285**, 977.
- Nadassy, K., S. J. Wodak, and J. Janin, 1999, *Structural Features of Protein-Nucleic Acid Recognition Sites*, Biochemistry **38**, 1999.
- Park, C. S., Z. Hillel, and C. W. Wu, 1982a, *Molecular mechanism of promoter selection in gene transcription. I.*, J. Biol. Chem. **257**, 6944.
- Park, C. S., F. Y. Wu, and C. W. Wu, 1982b, *Molecular mechanism of promoter selection in gene transcription. II.*, J. Biol. Chem. **257**, 6950.
- Place, C. *et al.*, 2001, work in progress at the Physics Laboratory, E.N.S., Lyon.
- Ricchetti, M., W. Metzger, and H. Heumann, 1988, *One-dimensional diffusion of Escherichia coli DNA-dependent RNA polymerase: A mechanism to facilitate promoter location*, Proc. Natl. Acad. Sci. U.S.A. **85**, 4610.
- Salerno, M., 1991, *Discrete model for DNA promoters dynamics*, Phys.Rev. A **44**, 5292.
- Salerno, M., 1995, in *Nonlinear Excitations in Biomolecules*, edited by M. Peyrard (Edition de Physique, Springer), p. 147.
- Schulz, A. *et al.*, 1998, *Scanning Force Microscopy of Escherichia coli RNA Polymerase sigma 54 Holoenzyme Complexes with DNA Buffer and in Air*, J. Mol. Biol. **283**, 921.
- Seeman, N. C., J. M. Rosenberg, and A. Rich, 1976, *Sequence-specific recognition of double helical nucleic acids by proteins*, Proc. Natl. Acad. Sci. USA **73**, 804.
- Shimamoto, N., 1999, *One dimensional diffusion of proteins along DNA: its biological and chemical significance revealed by single-molecule measurements*, J. Biol. Chem. **274**, 15293.
- Singer, P. and C. W. Wu, 1987, *Promoter search by Escherichia coli RNA polymerase on a circular DNA template*, J. Biol. Chem. **262**, 14178.
- Stanford, N. *et al.*, 2000, *One- and three-dimensional pathways for proteins to reach specific DNA sites*, EMBO Journal **19**, 6546.
- Stryer, L., 1995, *Biochemistry* (W. H. Freeman and Company, Inc., New York).
- Travers, A., 1993, *DNA-Protein Interactions* (Chapman and Hall, London), chapter 3 and 4.
- Voet, D. and J. G. Voet, 1995, *Biochemistry* (John Wiley & Sons, New York).